

# Transport of exotic anti-nuclei: I- Fast formulae for $\bar{p}$ fluxes

D. Maurin<sup>a,b,\*</sup> R. Taillet<sup>c,d</sup> C. Combet<sup>e,f</sup>

<sup>a</sup>*Dipartimento di Fisica Teorica, Università di Torino, Istituto Nazionale di Fisica Nucleare, via P. Giuria 1, I-10125 Torino, Italy*

<sup>b</sup>*LPNHE, IN2P3/CNRS/Universités Paris VI et Paris VII, 4 place Jussieu Tour 33 - Rez de chaussée, 75252 Paris Cedex 05, France*

<sup>c</sup>*Laboratoire de Physique Théorique LAPTH, Annecy-le-Vieux, 74941, France*

<sup>d</sup>*Université de Savoie, Chambéry, 73011, France*

<sup>e</sup>*Dublin Institute for Advanced Studies DIAS, 5 Merrion Square, Dublin 2, Ireland*

<sup>f</sup>*Laboratoire d'Astrophysique, Observatoire de Grenoble LAOG, BP 53 F-38041 Grenoble Cedex 9, France*

---

## Abstract

The Galactic secondary cosmic ray anti-proton ( $\bar{p}$ ) flux calculated with different propagation models is fairly consistent with data, and the associated propagation uncertainty is small. This is not the case for any  $\bar{p}$  exotic component of the dark matter halo (see also the companion paper; Maurin et al. 2006). Detailed propagation models are mandatory if the ultimate goal is to explain an excess. However, simpler and faster approximate formulae for  $\bar{p}$  are an attractive alternative to quickly check that a given dark matter model is not inconsistent with the  $\bar{p}$  observed flux. This paper provides such formulae. In addition, they could be used to put constraints on new physics in this channel, where an extensive scan of a large parameter space could otherwise be quite expensive in computer resources.

*Key words:* Cosmic Rays, Diffusion equation, Anti-nuclei, Dark matter, Indirect detection

*PACS:* 98.38.Cp, 98.35.Pr, 96.40.-z, 98.70.Sa, 96.50S-, 96.50sb, 95.30.Cq, 12.60.Jv, 95.35.+d

---

## 1. Motivation

The first positive detection of anti-protons at the end of the seventies (Golden et al., 1979; Buffington et al., 1981; Bogomolov et al., 1982) boosted the interest for indirect searches of new physics in the low energy  $\bar{p}$  spectrum. After 25 years of efforts and improvements both in measurements and theoretical calculations, the data at low energy (up to a few GeV) are now well accounted for (Donato et al., 2001). However, at higher energy, calculations tend to predict less  $\bar{p}$  than observed (Boezio et al., 2001) but more data are desirable to confirm this possible trend.

The uncertainty of the  $\bar{p}$  standard secondary flux (Donato et al., 2001) mainly comes from nuclear physics, as that of astrophysical origin is small—less than a few percents—and is expected to decrease even more as new B/C measurements are available. In contrast, the  $\bar{p}$  exotic flux—from exotic sources following the dark matter distribution—is plagued by the degeneracy in the prop-

agation parameters, the corresponding uncertainty being as large as two orders of magnitude at low energy (Donato et al., 2004). Until propagation is better understood and constrained, it may not be worth using refined—and sometimes time consuming—models whose result will anyway be crippled by these large uncertainties. This is especially true when one has to scan as efficiently as possible the huge parameter space existing, for example, in SUSY theories.

The goal of this paper is to provide approximate formulae for the propagated  $\bar{p}$  exotic fluxes. This is done in the framework of the diffusion/convection model with constant wind already discussed in Maurin et al. (2001); Donato et al. (2001); Barrau et al. (2002); Donato et al. (2004). These formulae are reasonably accurate, fast to compute and easy to implement. They have to be thought as an easy-to-use tool, for phenomenologists interested in beyond-the-standard-model theories and wishing to quickly check that any new physics model on the market does not violate the  $\bar{p}$  constraint. Once the interesting regions of the parameter space (for the dark matter candidate) are identified, more elaborate treatments should be implemented (e.g. GALPROP—Moskalenko et al. 2005; DARKSUSY—Gondolo et al. 2004; or Donato et al. 2004).

---

\* Corresponding author.

*Email addresses:* dmaurin@lpnhe.in2p3.fr (D. Maurin),

taillet@lapp.in2p3.fr (R. Taillet),

ccombet@obs.ujf-grenoble.fr (C. Combet).

The paper is organized as follows:

- In Sec. 2, we remind the salient ingredients of the constant wind/diffusion model for secondary and primary exotic anti-protons, using a Bessel expansion formalism.
  - In Sec. 3, two alternative formulations of the  $\bar{p}$  primary exotic flux are presented.
  - In Sec. 4, all the formulations are compared and their relative merits discussed.
- The formulae given in Sec. 3 are implemented in numerical routines publicly available<sup>1</sup>.

## 2. 2D-model with constant wind $V_c$

Cosmic ray fluxes are determined by the transport equation, as given, e.g., in Berezhinskii et al. (1990). Throughout the paper, we use the so-called thin-disk approximation where the gas is contained in a layer of thickness  $2h = 200$  pc. Cylindrical symmetry is assumed, and the diffusion coefficient is constant in the whole Galaxy,

$$K(E) = \beta K_0 \mathcal{R}^\delta \quad (\mathcal{R} = pc/|Z|e \text{ is the rigidity}).$$

A galactic wind  $V_c$  of constant magnitude, directed outwards along  $z$ , is also included.

### 2.1. Diffusion equation

Denoting the differential density as  $N$  leads to

$$\begin{aligned} & \left\{ -K\Delta + V_c \frac{\partial}{\partial z} + 2h\Gamma_{\text{tot}}\delta(z) \right\} N \\ & + 2h\delta(z) \left[ b(E) \frac{dN}{dE} + c(E) \frac{d^2 N}{dE^2} \right] \\ & = \mathcal{S}(r, z, E). \end{aligned} \quad (1)$$

The quantity  $\Gamma_{\text{tot}} = \sum_{\text{ISM}} n_{\text{ISM}} \cdot v \cdot \sigma_{\text{ISM}}^{\bar{p}}$  is the destruction rate of  $\bar{p}$  in the thin gaseous disk ( $n_{\text{ISM}} = \text{H, He}$ ). The terms  $b(E)$  and  $c(E)$  correspond respectively to a drift term (coulomb, ionization, adiabatic losses and reacceleration) and a diffusion term (reacceleration depending on the Alfvénic velocity) in energy space (e.g., Maurin et al. 2001, 2002). The quantity  $\mathcal{S}(r, z, E)$  stands for the source term and has three contributions: secondary (spallation-induced), tertiary (non-annihilating rescattering) and primary (exotic dark matter)—Donato et al. (2001, 2004). In the remaining of the paper, we term *energy redistribution* the effects of drift, diffusion and tertiary contribution.

### 2.2. Propagation parameters

The parameters of the model relevant to the present study are i) the size  $L$  of the diffusive halo of the Galaxy, ii) the normalization of the diffusion coefficient  $K_0$ , iii) its slope  $\delta$  and iv) the constant galactic wind  $V_c$ . The boundary conditions are  $N(z = L, r) = 0$  and  $N(r = R, z) = 0$ , where

Set	$\delta$	$K_0$ (kpc <sup>2</sup> Myr <sup>-1</sup> )	$L$ (kpc)	$V_c$ (km s <sup>-1</sup> )
<i>max</i>	0.46	0.0765	15	5
<i>best</i>	0.7	0.0112	4	12
<i>min</i>	0.85	0.0016	1	13.5

Table 1

Propagation parameters consistent with B/C data (Maurin et al., 2001). The set labeled *best* corresponds to the best fit to B/C data, while those labeled *min* and *max* correspond to sets which give minimum and maximum exotic fluxes (Donato et al., 2004).

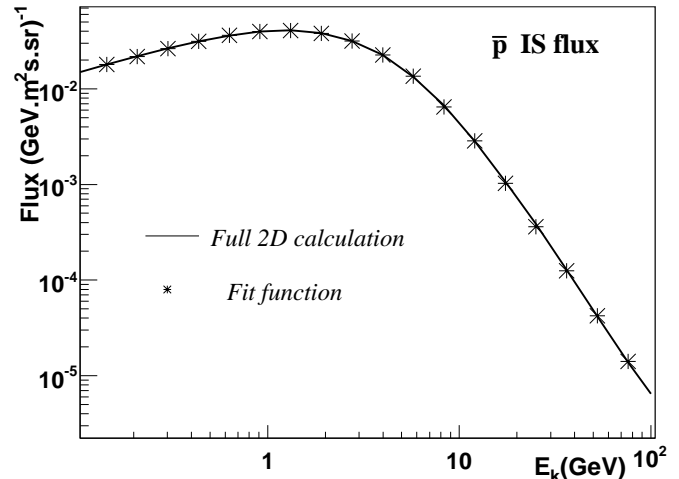


Fig. 1. Reference interstellar standard  $\bar{p}$  flux along with its fit function as given by Eq. (2).

the Galactic radius is  $R = 20$  kpc. The propagation parameters have been determined from the analysis of the B/C ratio in Maurin et al. (2001): only a sub-region of the propagation parameter space is compatible with B/C data. The accuracy of the approximate formulae given in this work is studied for this sub-region only. Within the latter, the sets of parameters leading to the maximum/minimum primary exotic fluxes (see Donato et al. 2004 and the companion paper) are gathered in Tab. 1, along with the configuration corresponding to the best fit to B/C data. These three sets were previously used in Donato et al. (2004); Barrau et al. (2005).

### 2.3. Secondary $\bar{p}$ flux

The secondary  $\bar{p}$  flux has been studied in detail in Donato et al. (2001): every set of propagation parameters consistent with the observed B/C ratio leads to the same  $\bar{p}$  secondary flux, within the  $\sim 10\%$  uncertainties mostly of nuclear origin. Moreover, the  $\bar{p}$  fluxes obtained from other models are in fair agreement (see e.g. Moskalenko et al. 2002).

If one wishes to exclude, for example, an exotic primary contribution by scanning the SUSY parameter space, it is useless to calculate again and again the same quantity with various input propagation parameters. The following fit function, once modulated, provides a proper description of the measured  $\bar{p}$  secondary flux, regardless of the propa-

<sup>1</sup> [http://wwwlapp.in2p3.fr/~taillet/mtc/mtc\\_code.tar](http://wwwlapp.in2p3.fr/~taillet/mtc/mtc_code.tar)

gation model. Setting  $x \equiv \log(E_k)$  where  $E_k$  is the kinetic energy in GeV, the standard IS  $\bar{p}$  flux in  $(\text{GeV m}^2 \text{ s sr})^{-1}$  is parameterized as

$$\Phi_{\text{standard}}^{\bar{p} - \text{IS}} = \begin{cases} \exp\left(\sum_{i=0}^4 C_i x^i\right) & \text{if } E_k < 11 \text{ GeV}, \\ \exp(D_0 x^{D_1}) & \text{otherwise;} \end{cases} \quad (2)$$

The constants are defined by  $C_0 = -3.211$ ,  $C_1 = 0.12145$ ,  $C_2 = -0.2728$ ,  $C_3 = -0.075265$ ,  $C_4 = -0.007162$ , and  $D_0 = -2.02735$  and  $D_1 = 1.16463$ . The fit is shown in Fig. 1.

#### 2.4. Exotic primary $\bar{p}$ flux

The derivation for the primary flux has been presented in Barrau et al. (2002)<sup>2</sup>. The solution can be found using a Bessel expansion (see e.g., Maurin et al. 2001)

$$N^{\text{prim}}(r, z) = \sum_{i=1}^{\infty} \mathcal{N}_i^{\text{prim}}(z) J_0\left(\zeta_i \frac{r}{R}\right),$$

where  $\zeta_i$  is the  $i$ -th zero of  $J_0$  and

$$\begin{aligned} \mathcal{N}_i^{\text{prim}}(z) = & \mathcal{N}_i(0) e^{\frac{V_c z}{2K}} \frac{\sinh\left[\frac{S_i}{2}(L-z)\right]}{\sinh\left(\frac{S_i L}{2}\right)} \\ & + e^{-\frac{V_c}{2K}(L-z)} \frac{\sinh(S_i z/2)}{\sinh(S_i L/2)} \frac{y_i(L)}{K S_i} - \frac{y_i(z)}{K S_i}. \end{aligned} \quad (3)$$

Each  $\mathcal{N}_i(0)$  obeys a differential equation

$$\mathcal{N}_i(0) = \mathcal{N}_i^*(0) - \frac{2h}{K} \left[ b(E) \frac{d\mathcal{N}_i(0)}{dE} + c(E) \frac{d^2 \mathcal{N}_i(0)}{dE^2} \right], \quad (4)$$

where  $\mathcal{N}_i^*(0)$  is the solution without energy redistributions:

$$\mathcal{N}_i^*(0) \equiv e^{-V_c L/2K} \frac{y_i(L)}{A_i \sinh(S_i L/2)}. \quad (5)$$

Equation (4) is solved with a numerical scheme detailed in Donato et al. (2001). The tertiary contribution is not shown in the former equation although it is taken into account in our numerical calculations. The remaining quantities are defined as follows:

$$\begin{aligned} y_i(z) \equiv & 2 \int_0^z e^{\frac{V_c}{2K}(z-z')} \sinh\left[\frac{S_i}{2}(z-z')\right] q_i(z') dz'; \\ S_i \equiv & \sqrt{\frac{V_c^2}{K^2} + 4 \frac{C_i^2}{R^2}}; \quad A_i \equiv 2h\Gamma_{\text{tot}} + V_c + K S_i \coth\left(\frac{S_i L}{2}\right). \end{aligned}$$

In the above expression,  $q_i(z)$  are the Fourier-Bessel coefficients of the source term  $\mathcal{S}_{\text{prim}}(r, z)$ . Some numerical issues about the convergence of the series, when using cuspy dark matter halo, are underlined in App. B.

Halo model	$\alpha$	$\beta$	$\gamma$	$r_c$ [kpc]
Cored isothermal	2	2	0	4
NFW (Navarro et al., 1997, 2004)	1	3	1	25
Moore (Moore et al., Diemand et al.)	1	3	1.2	30

Table 2

Parameters to be plugged into Eq. (7) to obtain various modelings of the dark matter distribution profile in the Milky Way.

#### 2.5. Dark matter profile

The primary exotic source term follows the generic form

$$\mathcal{S}_{\text{prim}}(r, z) = Q^{\bar{p}}(E) \times f_{\text{Source}}(r, z), \quad (6)$$

where the spatial dependence of the source term is normalized to 1 at Solar position. For evaporation of Primordial Black Holes or for SUSY-like particles,  $f_{\text{Source}}(r, z)$  is equal to

$$f_{\text{Dark}}(r, z) \quad \text{or} \quad f_{\text{Dark}}^2(r, z),$$

where  $f_{\text{Dark}}(r, z)$  is the dark matter distribution profile, also normalized to 1 at Solar position. Any information such as, e.g., the relic density, the fraction of the dark matter halo filled by the new candidate or any quantity related to the dark matter candidate is irrelevant at this stage: it is absorbed in the energy dependent term  $Q(E)$ . The right factors should be implemented accordingly when using the approximate formulae.

The following generic form is taken for the profile:

$$f_{\text{Dark}}(r, z) = \left(\frac{R_{\odot}}{\sqrt{r^2 + z^2}}\right)^{\gamma} \left(\frac{r_c^{\alpha} + R_{\odot}^{\alpha}}{r_c^{\alpha} + \sqrt{r^2 + z^2}^{\alpha}}\right)^{(\beta-\gamma)/\alpha}, \quad (7)$$

where parameters are given in Tab. 2. The distance to the galactic center is set to  $R_{\odot} = 7.5$  kpc, a value that several methods seem to converge to (Nishiyama et al., 2006). This is at variance with the usually recommended  $R_{\odot} = 8.0$  kpc (e.g. Yao et al. 2006), but has no impact on the derived results below. Indeed,  $R_{\odot}$  is just another parameter, and our approximate formulae will perform well for any user-preferred value  $\approx 8.0$  kpc.

### 3. Approximate formulae

The previous formulae (see Sec. 2.4) can be tricky to implement in practice (numerical inversion, tertiary contribution, convergence issues), especially when energy redistributions are included. In this section, energy gains and losses are discarded and a simplified formalism is presented for the calculation of exotic primary  $\bar{p}$  fluxes. Some of the formulae given hereafter are well suited for extensive computation.

#### 3.1. Propagator (no side boundaries: $R \rightarrow \infty$ )

In Taillet et al. (2004), the expression for the propagator corresponding to the same 2D diffusion equation (without

<sup>2</sup> Footnote that there is a misprint in Eq. (A.5) of (Barrau et al., 2002). The product  $K A_i S_i$  should read  $K S_i$ .

energy redistributions) was extracted in the limit  $^3 R \rightarrow \infty$ . Hence, the problem is invariant under radial translations and we choose the location of the observer as the origin ( $\mathbf{r} = \mathbf{0}$ ). The propagator  $\mathcal{G}(\mathbf{r} - \mathbf{r}')$  is solution of

$$\left\{ -K\Delta + V_c \frac{\partial}{\partial z} + 2hn\delta(z)v\sigma \right\} \mathcal{G} = \delta(\mathbf{r} - \mathbf{r}')$$

and reads (see App. A)

$$\mathcal{G}(r, z) = \frac{\exp^{-k_v z}}{2\pi KL} \times \sum_{n=0}^{\infty} c_n^{-1} K_0(r\sqrt{k_n^2 + k_v^2}) \sin k_n L \sin k_n(L - z) \quad (8)$$

where  $K_0$  is the modified Bessel function of the second kind,  $k_n$  is solution of

$$2k_n \cos k_n L = -k_d \sin k_n L, \quad (9)$$

$c_n$  is defined as

$$c_n = 1 - \frac{\sin k_n L \cos k_n L}{k_n L} \quad (10)$$

and

$$k_v \equiv V_c / (2K).$$

The quantity  $k_d$  depends on the total destruction rate  $\Gamma_{\text{tot}}$  and the constant convective wind  $V_c$ :

$$k_d \equiv 2h \Gamma_{\text{tot}} / K + 2k_v. \quad (11)$$

The flux at solar location is given by

$$N_{\odot} = 2 \int_0^{2\pi} \int_0^L \int_0^R \mathcal{G}(r, \theta, z) \mathcal{S}_{\text{prim}}(r, \theta, z) r d\theta dr dz.$$

where  $\mathcal{S}_{\text{prim}}(r, \theta, z)$  is the dark matter source term as seen from the Solar System. Hence, a single (numerical) integration is needed in the propagator approach: this represents a great benefit compared to the full 2D description given in Sec. 2.

### 3.2. The 1D model

Another way to tackle the simplified problem (neglecting energy redistributions) is the use of a 1D model. We now consider an infinite disk whose density and source distribution do not depend on  $r$ . The constant wind diffusion transport equation for a generic source term  $\mathcal{Q}(z, E) = q(z)Q(E)$  without energy redistributions reads

$$-K \frac{d^2 N}{dz^2} + V_c \frac{dN}{dz} + 2h\delta(z)\Gamma_{\text{tot}} N = q(z)Q(E). \quad (12)$$

As we do not take into account energy losses, the energy  $E$  is decoupled from the spatial dependence  $z$  so that it

<sup>3</sup> The propagator for finite  $R$  was presented and used in Maurin and Taillet (2003) to obtain the most likely *origin* of exotic  $\bar{\nu}$  detected on Earth. This propagator relied on Bessel expansion. For practical use,  $R \gg 1$  was required, so that it was equivalent to the form presented below. However, in the context of a quick and simple formulae, it is largely outperformed (in term of convergence properties) by the one presented in this paper.

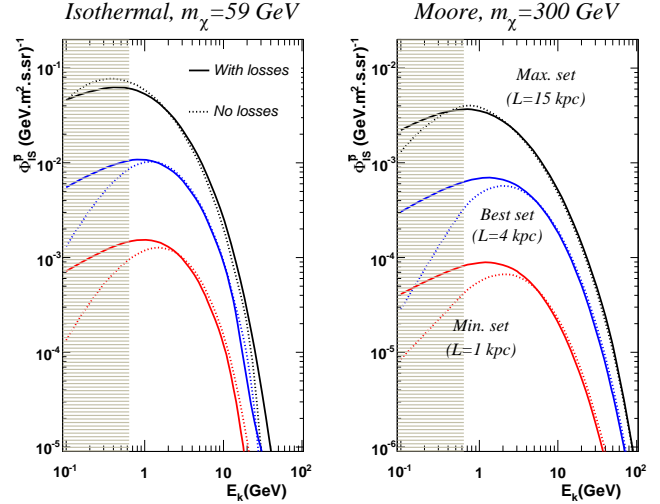


Fig. 2. From top to bottom, the *max*, *best* and the *min* propagation sets (see Tab. 1). The dashed lines correspond to the propagated fluxes without energy redistributions, while solid lines correspond to the same propagated exotic fluxes, but with energy redistributions (energy losses, reacceleration, tertiary source term) taken into account. The shaded regions correspond to  $\bar{\nu}$  which cannot reach Earth (because of solar modulation, see text). The two panels correspond to different dark matter profiles and neutralino masses.

is omitted. In 1D-models, only  $z$ -dependence is allowed. For simplicity, it is further assumed that the source term  $q$  is constant throughout the Galaxy. We refer the reader to the companion paper for details of the calculation. The analytical solution reads

$$\begin{cases} N(z) = \frac{qL}{V_c} \left\{ \frac{(1 + \alpha + \xi) \cdot (1 - e^{-\alpha(1 - \frac{z}{L})})}{\alpha + \xi(1 - e^{-\alpha})} + \frac{z}{L} - 1 \right\} \\ N(0) = \frac{qL}{V_c} \left\{ \frac{1 - (1 + \alpha)e^{-\alpha}}{\alpha + \xi(1 - e^{-\alpha})} \right\} \end{cases} \quad (13)$$

where  $\xi = h\Gamma_{\text{tot}}L/K$  and  $\alpha = V_cL/K$ .

## 4. Results

In this section, the validity of the previous approximate formulae is checked. We first study the influence of energy redistributions within the 2D numerical framework and then compare the two simplified formulae to the 2D numerical model (without energy redistributions).

### 4.1. Influence of energy redistributions in the 2D model

The realistic dark matter profile (as described in Sec. 2.5) is implemented in the full 2D-model (see Sec. 2.4), with and without energy redistributions. When energy redistributions are neglected, the quantity  $\mathcal{N}_i(0)$  to plug in Eq. (3) becomes the quantity  $\mathcal{N}_i^*(0)$  defined in Eq. (5). We use the generic term *error* for the difference between solutions calculated with and without energy redistributions.

#### 4.1.1. Expected effect of energy redistributions

As energy redistributions act on the spectrum, it is not obvious to disentangle which of the following input parameters—source spectrum, profile, transport coefficients—is the most crucial regarding *error*. On a general footing, energy losses and tertiary contributions tend to replenish the low energy tail in case of a dropping flux at these same energies (this has a particularly important impact on the standard secondary  $\bar{p}$ , see Donato et al. 2001). On the other hand, reacceleration tends to smear the spectrum at low and high energy in case of a flux peaking at GeV energy. Taking all these points into account, the following remarks—regarding energy redistributions—can be made:

**Source spectrum:** in most cases, PBH-like source spectra do not decrease at low energy (e.g., Fig. 3 of Barrau et al. 2002), whereas SUSY-like candidates are quite flat (e.g., Fig. 6 of Donato et al. 2004). Hence, taking various source spectra is not expected to play a major role in *error*.

**Dark matter profile:** changing the spatial distribution does not affect the spectral distribution: it only changes the normalization of the propagated spectrum. Hence, no significant effect on *error* is expected when switching between SUSY-like to PBH-like source terms.

**Propagation parameters:** Large winds dominate over diffusion as the energy diminishes: they decrease low energy fluxes, making them more sensitive to energy redistribution effects. These large wind happen to be associated with a small halo size and a small reacceleration parameter. This effect is larger than the two others (see below).

#### 4.1.2. Behavior of error

Figure 2 displays the two resulting fluxes for various input configurations. The decrease of the flux observed at low energy for the best and minimal propagation sets is due to the Galactic wind. For the smallest  $L$ , the propagated flux is steeper (because of larger wind values, see Tab. 1), hence more affected by energy redistributions. Notice that only for  $L = 15$  kpc (corresponding to  $V_c = 5$  km s $^{-1}$ ), can the shape of the source spectrum be truly appreciated. As expected, the *error* calculated when varying the neutralino mass or the dark matter profile is less important.

The *error* can be as large as a factor of  $\sim 5$  at very low energy, but we remind that these are  $\bar{p}$  at IS energies, which cannot reach Earth because of solar modulation (shaded region in Fig. 2). Indeed, the top of atmosphere energy  $E_{\text{TOA}}$  is related to the interstellar energy  $E_{\text{IS}}$  by  $E_{\text{IS}} = E_{\text{TOA}} + \phi$  where  $\phi$  is the modulation parameter  $\in [500 - 1000]$  MV (Perko, 1987).

Above a few hundreds of MeV (lowest IS energy reachable for low solar activity), the difference obtained is always  $\lesssim 50\%$ . Above a few tens of GeV, energy redistributions are always negligible, so that *error* tends to zero. In between, the only situation when *error* can be large corre-

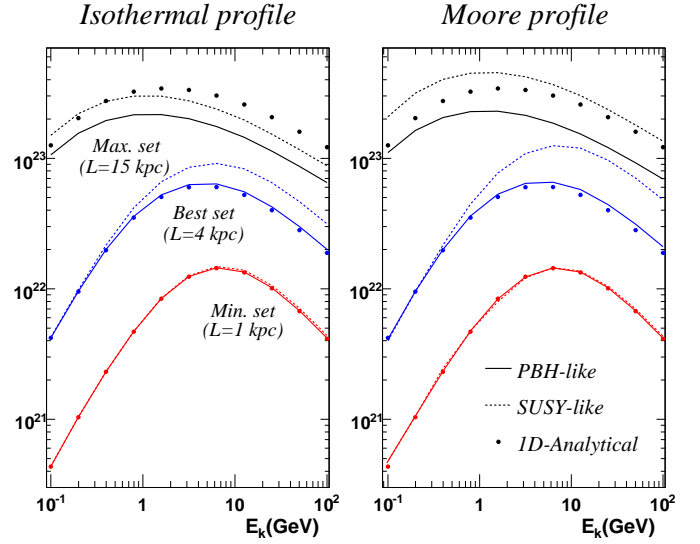


Fig. 3. Both figures correspond to the ratio of the  $\bar{p}$  exotic flux to its source term (in arbitrary units) as a function of the kinetic energy. Lines: 2D—semi-analytical model, no energy redistributions (Sec. 2.4) for PBH-like (solid lines) or SUSY-like (dashed lines) sources. Symbols: Eq. (13), 1D—model (independent of the dark matter profile). The three sets of propagation parameters are those of Tab. 1. Left panel: Isothermal profile; right panel: Moore profile.

sponds to a steep spectrum dropping rapidly to zero, which is uninteresting in the perspective of detecting any excess.

#### 4.1.3. Summary

The model neglecting energy redistributions is accurate enough to determine exotic fluxes. This result is in agreement with the intuitive idea that exotic species, in order to reach us, cross the gaseous disk less often than standard ones, implying that they are less subject to energy redistributions.

### 4.2. Approximate formulae vs 2D reference model

#### 4.2.1. Propagator

As expected, the propagator (see Sec. 3.1) and the Bessel expansion (see Sec. 2.4) formalisms are consistent, except when the halo size has the same extension of the radial extension of the Galaxy  $R$ . In that case, we no longer have  $L \ll R$  and the side boundary starts affecting the flux, as discussed in (Taillet and Maurin, 2003; Maurin and Taillet, 2003).

#### 4.2.2. 1D—model

Figure 3 compares the 1D—model (at  $z = 0$ ) to the 2D semi-analytical model:

- For PBH-like sources, as long as  $L \lesssim 7$  kpc, the 1D—model provides a good description of exotic  $\bar{p}$  fluxes.
- For SUSY-like sources, 1D—models are valid for very small halo size  $L$  only.

This good agreement is easily understood if we remember that the closest boundary defines a cut-off distance: anti-nuclei from sources located further away are exponentially

suppressed (Taillet and Maurin, 2003; Maurin and Taillet, 2003). Hence, we are only sensitive to the average value of  $f_{\text{Dark}}$  within this cut-off distance, close to one at solar position, as taken in the 1D-model. As soon as contributions close to the Galactic center are less suppressed, this equivalence breaks down; all the more for SUSY-like source terms compared to PBH-like source terms (because of the square in  $f_{\text{Dark}}$ ).

## 5. Numerical routines

Taking advantage of the two simplified formalisms depicted above (propagator and 1D model), routines are provided<sup>4</sup>, to evaluate the  $\bar{p}$  flux from any input dark matter profile, source spectrum, and propagation parameters. The main routine returns the ratio of the propagated IS exotic flux (for a user-specified source term) to the standard  $\bar{p}$  IS flux, i.e.

$$\mathcal{U} \equiv \Phi_{\text{exotic}}^{\bar{p} \text{ -IS}} / \Phi_{\text{standard}}^{\bar{p} \text{ -IS}} .$$

The input parameters are the following:

- Propagation parameters:  $K_0$  ( $\text{kpc}^2 \text{ Myr}^{-1}$ ),  $\delta$ ,  $V_c$  ( $\text{km s}^{-1}$ ) and  $L$  ( $\text{kpc}$ );
- Exotic source spectrum:  $Q_{\text{exotic}}^{\bar{p}}(E_k)$  ( $\text{GeV}^{-1} \text{ m}^{-3} \text{ s}^{-1}$ ) and the corresponding kinetic energy  $E_k$  ( $\text{GeV}$ );
- Dark matter profile: the parameters  $\alpha$ ,  $\beta$  and  $\gamma$  (see 2) as well as the source type (SUSY-like or PBH-like).

The resulting fluxes, in  $(\text{GeV m}^2 \text{ s sr})^{-1}$ , are obtained at solar position  $(R_{\odot}, 0)$ . The IS background  $\bar{p}$  spectrum is described using a fit function (see Sec. 2.3). We chose to express all fluxes as IS quantities to free the user from using a modulation routine. There are uncertainties associated with the choice of the modulation/demodulation scheme, but these are not larger than the error made using approximate formulae (see Moskalenko et al. 2002 for a discussion on solar modulation).

We remind that the range of propagation parameters given in Tab. 1 implies that large uncertainties remain on exotic fluxes (without mentioning the fact that the constant wind model is probably not the *definitive* model for the Galaxy). To make conservative estimates, we recommend the reader to use the *min* set of propagation parameters associated with the condition  $\mathcal{U} \gtrsim 1$  to exclude an exotic model. Regarding the most likely  $\bar{p}$  exotic flux in this model, it is given by the *best* set ( $L = 4 \text{ kpc}$ , see Tab. 1). In any case, it has to be kept in mind that energy smaller than  $\sim 600 \text{ MeV}$  IS correspond to  $\bar{p}$  which are almost never detected on Earth.

## 6. Conclusion

Given the present accuracy of propagation parameters, exotic anti-proton fluxes suffer large uncertainties (see also the companion paper). This limits the benefit of a detailed

calculation, which can be expensive in term of computational power, when repeated thousands of times.

We showed that discarding energy redistributions (coulomb, ionization, adiabatic losses, reacceleration and tertiary contribution) provides exotic  $\bar{p}$  fluxes accurate at the level of  $\lesssim 50\%$  for IS energies greater than  $\sim 1 \text{ GeV}$  (leading to  $\gtrsim 100 \text{ MeV}$  energies once modulated). This opens the possibility to use one of the following simpler formulae:

- the approximate 1D-model, which gives the correct flux as long as  $L \lesssim 7 \text{ kpc}$  for PBH-like sources, or  $L \lesssim 1 \text{ kpc}$  for SUSY-like sources;
- the 2D-propagator.

The advantage of the 1D-model is its compactness and simplicity (no dependence on the dark matter profile), while the second approach is more accurate. The former could be preferred in situations where speed is a decisive factor, e.g. when scanning a large parameter space as in SUSY studies. Moreover, in order to be conservative in exclusion studies, small halo size should be taken. In particular conservative estimates are made when using the 3<sup>rd</sup> line of Tab. 1: this is exactly the regime where 1D-formulae hold. We also supply numerical routines that could be easily implemented in indirect detection codes.

So far, these formulae are valid only in the framework of the constant wind model. Although all the discussions were developed with respect to exotic  $\bar{p}$  fluxes, all the results can be transposed almost without any modification to the  $\bar{d}$  case (the total cross section has to be taken accordingly to the species considered).

Acknowledgments We thank E. Nezri for useful discussions held during the GDR-SUSY meeting, and J. Lavalle and F. Donato for a careful reading of the manuscript.

## Appendix A. Check of propagator formulae

The validity of the propagator is checked in a simple case, by integrating it over a constant source term  $q(r, z) = 1$  (1D formula).

A.1. *Purely diffusive regime:  $V_c = 0$*

A.1.1. *No spallations,  $k_d = 0$*

In that case,  $k_n \equiv (n + 1/2)\pi$ . Integration over  $z$  (using  $q(r, z) = 1$ ) leads to

$$\int_{-L}^L dz \mathcal{G}(r, z) = \frac{1}{\pi K L} \sum_{n=0}^{\infty} \frac{(-1)^n}{k_n} K_0(k_n r) , \quad (\text{A.1})$$

and integration over the disk  $\int_0^R 2\pi r dr$  gives

$$N(0) = \frac{2}{K L} \sum_{n=0}^{\infty} \frac{(-1)^n}{k_n^3} \int_0^{k_n R} y K_0(y) dy .$$

<sup>4</sup> [http://wwwlapp.in2p3.fr/~taillet/mtc/mtc\\_code.tar](http://wwwlapp.in2p3.fr/~taillet/mtc/mtc_code.tar)

Using the properties  $\int y K_0(y) dy = -yK_1(y)$  and  $yK_1(y) \sim 1$  when  $y \rightarrow 0$ ,

$$N(0) = \frac{2}{KL} \sum_{n=0}^{\infty} \frac{(-1)^n}{k_n^3} [1 - k_n R K_1(k_n R)] .$$

Finally, for  $R \gg 1$ , the expression becomes

$$N(0) = \frac{2}{KL} \sum_{n=0}^{\infty} \frac{(-1)^n}{k_n^3} = \frac{2L^2}{\pi^3 K} \sum_{n=0}^{\infty} \frac{(-1)^n}{(n+1/2)^3} .$$

The infinite sum has the value  $\sum (-1)^n / (n+1/2)^3 = \pi^3/4 \approx 7.7515$ , so that

$$N(0) = \frac{L^2}{2K} \equiv N^{\text{1D-model}}(0) .$$

Note that, in the infinite sum, the first term  $n=0$  is equal to 8, so that it only slightly overshoots the exact value. Hence, only a few terms are required in the sum to converge quickly to the correct value.

#### A.1.2. With spallations, $k_d = 2h\Gamma_{\text{tot}}/K$

There is no longer a simple expression for  $k_n$ . Following a similar derivation as the one above, we find

$$N(0) = \frac{4}{Kk_dL} \sum_{n=0}^{\infty} \left( 1 - \frac{\sin k_n L \cos k_n L}{k_n L} \right)^{-1} \times \frac{\cos k_n L}{k_n^2} [\cos k_n L - 1] . \quad (\text{A.2})$$

A numerical check of this sum confirms that Eq. (A.2) equals the 1D-model, i.e. Eq. (13) where  $V_c = 0$ . This means that

$$\sum_{n=0}^{\infty} \frac{\cos(k_n L) [\cos(k_n L) - 1]}{k_n L (k_n L - \sin(k_n L) \cos(k_n L))} = \frac{k_d L}{4(2 + k_d L)} .$$

#### A.2. Diffusive/convective regime: $V_c \neq 0$

The integration leads to quite similar results as for the previous case (with spallations). A numerical check confirms that Eq. (13) is recovered.

Note that the integration should be performed for sources located at all  $r$ , with  $r \rightarrow \infty$ . In practice, it is sufficient (and it saves a lot of computational time) to integrate only from 0 to  $10L$  (or from 0 to  $\min(10L, 10L_{\text{eff}})$ ) in the case of a convective wind, where  $L_{\text{eff}} \equiv K/V_c$ . In that case, a grid of  $\sim 25$  points for all coordinates ( $r$ ,  $z$  and  $\theta$ ) is sufficient to reach the correct result.

### Appendix B. Numerical instabilities in the 2D model

Dealing with Bessel functions is a source of numerical instabilities. These occur if i)  $R \gg L$  or ii) too many Bessel orders are used, or even, in the case of cuspy dark matter halo, if too few orders are used. As the propagator formulation allows cross-checks, we take the opportunity to give a few recommendations regarding the parameters to use:

- (i) always keep  $R$  in the range  $5L^* \lesssim R \lesssim 10L^*$ , with  $L^* = \min(L, K/V_c)$ . The limit  $10L^*$  is set to avoid numerical instabilities while the limit  $5L^*$  allows to avoid boundary effects (Maurin and Taillet, 2003) (the boundary in  $R$  decreases the flux at most to a few tens of percent for a Moore profile).
- (ii) For a smooth profile (e.g. Isothermal), 20 Bessel functions give an excellent convergence.
- (iii) For NFW and Moore profiles in the case of SUSY-like candidate (50 Bessel functions are sufficient for PBH-like candidate), following a procedure inspired by Barrau et al. (2005), we replace in the calculation the standard profile, by

$$g_{\text{Dark}}^2(r) = \begin{cases} r_{\text{th}}^{2\gamma} \cdot f_{\text{Dark}}^2(r_{\text{th}}) \cdot \pi^2 \Upsilon \cdot \frac{\sin(\pi r/r_{\text{th}})}{\pi r/r_{\text{th}}} & \text{if } r \leq r_{\text{th}}; \\ f_{\text{Dark}}^2(r) & \text{otherwise;} \end{cases} \quad (\text{B.1})$$

with  $\Upsilon = (3-2\gamma)^{-1}$  and  $\gamma$  is the slope from Tab. 2. In these expressions,  $r \equiv \sqrt{r_{\text{cyl}}^2 + z^2}$  denotes the spherical coordinate. In any case, we find that, setting  $r_{\text{th}} = 400$  pc, 50 Bessel functions give a good accuracy, while 100 functions allow to reach an excellent convergence.

#### References

- Barrau, A., Boudoul, G., Donato, F., Maurin, D., Salati, P., Taillet, R., Jun. 2002. Antiprotons from primordial black holes. *Astronomy and Astrophys.* 388, 676–687.
- Barrau, A., Salati, P., Servant, G., Donato, F., Grain, J., Maurin, D., Taillet, R., Sep. 2005. Kaluza-Klein dark matter and galactic antiprotons. *Phys. Rev. D* 72 (6), 063507.
- Berezinskii, V. S., Bulanov, S. V., Dogiel, V. A., Ptuskin, V. S., 1990. *Astrophysics of cosmic rays*. Amsterdam: North-Holland, 1990, edited by Ginzburg, V.L.
- Boezio, M., Bonvicini, V., Schiavon, P., Vacchi, A., Zampa, N., Bergström, D., Carlson, P., Francke, T., Grinstein, S., Suffert, M., Hof, M., Kremer, J., Menn, W., Simon, M., Stephens, S. A., Ambriola, M., Bellotti, R., Cafagna, F., Ciaccio, F., Circella, M., De Marzo, C., Finetti, N., Papini, P., Piccardi, S., Spillantini, P., Vannuccini, E., Bartalucci, S., Ricci, M., Casolino, M., De Pascale, M. P., Morselli, A., Picozza, P., Sparvoli, R., Mitchell, J. W., Ormes, J. F., Streitmatter, R. E., Bravar, U., Stochaj, S. J., Nov. 2001. The Cosmic-Ray Antiproton Flux between 3 and 49 GeV. *Astrophys. Journal* 561, 787–799.
- Bogomolov, E. A., Lubianaia, N. D., Romanov, V. A., Stepanov, S. V., Shulakova, M. S., 1982. Galactic antiprotons of 2 - 5 GeV energy. In: *International Cosmic Ray Conference*. pp. 146–149.
- Buffington, A., Schindler, S. M., Pennypacker, C. R., Sep. 1981. A measurement of the cosmic-ray antiproton flux and a search for antihelium. *Astrophys. Journal* 248, 1179–1193.

- Donato, F., Fornengo, N., Maurin, D., Salati, P., Taillet, R., Mar. 2004. Antiprotons in cosmic rays from neutralino annihilation. *Phys. Rev. D* 69 (6), 063501.
- Donato, F., Maurin, D., Salati, P., Barrau, A., Boudoul, G., Taillet, R., Dec. 2001. Antiprotons from Spallations of Cosmic Rays on Interstellar Matter. *Astrophys. Journal* 563, 172–184.
- Golden, R. L., Horan, S., Mauger, B. G., Badhwar, G. D., Lacy, J. L., Stephens, S. A., Daniel, R. R., Zipse, J. E., Oct. 1979. Evidence for the existence of cosmic-ray antiprotons. *Physical Review Letters* 43, 1196–1199.
- Gondolo, P., Edsjö, J., Ullio, P., Bergström, L., Schelke, M., Baltz, E. A., Jul. 2004. DarkSUSY: computing supersymmetric dark matter properties numerically. *Journal of Cosmology and Astro-Particle Physics* 7, 8.
- Maurin, D., Donato, F., Taillet, R., Salati, P., Jul. 2001. Cosmic Rays below  $Z=30$  in a Diffusion Model: New Constraints on Propagation Parameters. *Astrophys. Journal* 555, 585–596.
- Maurin, D., Taillet, R., Jun. 2003. Spatial origin of Galactic cosmic rays in diffusion models. II. Exotic primary cosmic rays. *Astronomy and Astrophys.* 404, 949–958.
- Maurin, D., Taillet, R., Combet, C., 2006. Transport of exotic anti-nuclei. ii: anti-p and anti-d astrophysical uncertainties. [astro-ph/0612714](http://astro-ph/0612714).
- Maurin, D., Taillet, R., Donato, F., Nov. 2002. New results on source and diffusion spectral features of Galactic cosmic rays: I B/C ratio. *Astronomy and Astrophys.* 394, 1039–1056.
- Moskalenko, I. V., Strong, A. W., Ormes, J. F., Mashnik, S. G., 2005. Propagation of secondary antiprotons and cosmic rays in the Galaxy. *Advances in Space Research* 35, 156–161.
- Moskalenko, I. V., Strong, A. W., Ormes, J. F., Potgieter, M. S., Jan. 2002. Secondary Antiprotons and Propagation of Cosmic Rays in the Galaxy and Heliosphere. *Astrophys. Journal* 565, 280–296.
- Navarro, J. F., Frenk, C. S., White, S. D. M., Dec. 1997. A Universal Density Profile from Hierarchical Clustering. *Astrophys. Journal* 490, 493.
- Navarro, J. F., Hayashi, E., Power, C., Jenkins, A. R., Frenk, C. S., White, S. D. M., Springel, V., Stadel, J., Quinn, T. R., Apr. 2004. The inner structure of  $\Lambda$ CDM haloes - III. Universality and asymptotic slopes. *MNRAS* 349, 1039–1051.
- Nishiyama, S., Nagata, T., Sato, S., Kato, D., Nagayama, T., Kusakabe, N., Matsunaga, N., Naoi, T., Sugitani, K., Tamura, M., Aug. 2006. The Distance to the Galactic Center Derived from Infrared Photometry of Bulge Red Clump Stars. *Astrophys. Journal* 647, 1093–1098.
- Perko, J. S., Oct. 1987. Solar modulation of galactic antiprotons. *Astronomy and Astrophys.* 184, 119–121.
- Taillet, R., Maurin, D., May 2003. Spatial origin of Galactic cosmic rays in diffusion models. I. Standard sources in the Galactic disk. *Astronomy and Astrophys.* 402, 971–983.
- Taillet, R., Salati, P., Maurin, D., Pilon, E., 2004. Diffusion in a slab: different approaches. URL <http://www.citebase.org/abstract?id=oai:arXiv.org:physics/0405011>.
- Yao, W.-M., Amsler, C., Asner, D., Barnett, R., Beringer, J., Burchat, P., Carone, C., Caso, C., Dahl, O., D'Ambrosio, G., DeGouvea, A., Doser, M., Eidelman, S., Feng, J., Gherghetta, T., Goodman, M., Grab, C., Groom, D., Gurtu, A., Hagiwara, K., Hayes, K., Hernández-Rey, J., Hikasa, K., Jawahery, H., Kolda, C., Y., K., Mangano, M., Manohar, A., Masoni, A., Miquel, R., Mönig, K., Murayama, H., Nakamura, K., Navas, S., Olive, K., Pape, L., Patrignani, C., Piepke, A., Punzi, G., Raffelt, G., Smith, J., Tanabashi, M., Terning, J., Törnqvist, N., Trippe, T., Vogel, P., Watari, T., Wohl, C., Workman, R., Zyla, P., Armstrong, B., Harper, G., Lugovsky, V., Schaffner, P., Artuso, M., Babu, K., Band, H., Barberio, E., Battaglia, M., Bichsel, H., Biebel, O., Bloch, P., Blucher, E., Cahn, R., Casper, D., Cattai, A., Ceccucci, A., Chakraborty, D., Chivukula, R., Cowan, G., Damour, T., DeGrand, T., Desler, K., Dobbs, M., Drees, M., Edwards, A., Edwards, D., Elvira, V., Erler, J., Ezhela, V., Fetscher, W., Fields, B., Foster, B., Froidevaux, D., Gaisser, T., Garren, L., Gerber, H.-J., Gerbier, G., Gibbons, L., Gilman, F., Giudice, G., Gritsan, A., Grünewald, M., Haber, H., Hagemann, C., Hinchliffe, I., Höcker, A., Igo-Kemenes, P., Jackson, J., Johnson, K., Karlen, D., Kayser, B., Kirkby, D., Klein, S., Kleinknecht, K., Knowles, I., Kowalewski, R., Kreitz, P., Krusche, B., Kuyanov, Y., Lahav, O., Langacker, P., Liddle, A., Ligeti, Z., Liss, T., Littenberg, L., Liu, L., Lugovsky, K., Lugovsky, S., Mannel, T., Manley, D., Marciano, W., Martin, A., Milstead, D., Narain, M., Nason, P., Nir, Y., Peacock, J., Prell, S., Quadt, A., Raby, S., Ratcliff, B., Razuvaev, E., Renk, B., Richardson, P., Roesler, S., Rolandi, G., Ronan, M., Rosenberg, L., Sachrajda, C., Sarkar, S., Schmitt, M., Schneider, O., Scott, D., Sjöstrand, T., Smoot, G., Sokolsky, P., Spanier, S., Spieler, H., Stahl, A., Stanev, T., Streitmatter, R., Sumiyoshi, T., Tkachenko, N., Trilling, G., Valencia, G., van Bibber, K., Vincter, M., Ward, D., Weber, B., Wells, J., Whalley, M., Wolfenstein, L., Womersley, J., Woody, C., Yamamoto, A., Zenin, O., Zhang, J., Zhu, R.-Y., 2006. Review of Particle Physics. *Journal of Physics G* 33, 1. URL <http://pdg.lbl.gov>